Acta Polytechnica CTU Proceedings **54**:8–16, 2025
https://doi.org/10.14311/APP.2025.54.0008

Published by the Czech Technical University in Prague

CABLE OPTIMIZATION OF EXTRADOSED BRIDGES

Kristian D'Amico*, Jiří Máca

Czech Technical University in Prague, Faculty of Civil Engineering, Department of Mechanics, Thákurova 7, 166 29 Prague 6, Czech Republic

* corresponding author: kristian.d.amico@fsv.cvut.cz

Abstract. Extradosed bridges offer a competitive alternative to traditional systems used in spans ranging from 100 to 250 m. The trend in the world is the development of new materials and with it the design of thin structures, which is a challenging change for further development. Extradosed bridge is a relatively new type of construction (first in Odawara, Japan 1994), although there are many bridges of this type in the world, there are no strict design rules in terms of statics and even less in terms of dynamic behavior. To research this area closer, parametric analysis can be performed. Due to the complexity of this task and the non-linear coupling of the design parameters, it is necessary to approach it by an optimization method that, for predefined boundary conditions, optimizes the design response.

Keywords: Extradosed bridges, finite element method, optimization, non-linear cable analysis, tension stiffening, prestressing forces.

1. Introduction

The aim of this work is to create a tool for designing extradosed bridges and investigate the influence of structural parameters on the behaviour and efficiency of the structure. For arbitrary boundary conditions, the optimal distribution of forces in the cables can be found.

2. Extradosed bridges

Extradosed bridges with their shallow stay cables and stiff decks offer an economical and aesthetically pleasing alternative to conventional girder and cable-stayed bridges for spans within 100 and 250 meters (Figure 1). In an extradosed bridge the deck is partially supported by a system of cables anchored to relatively short pylons. Carrying the permanent loads of the bridge with such shallow inclined cables leads to high cable forces and high compression in the girder. At the anchorages, the horizontal components of these cable forces are introduced into the girder, thus contributing to its post-tensioning [1].

The shallow cables allow for very low heights and robust pylons, which are often placed in the centre of the girder (single cable plane), because the already strong box girder decks can also take torsional load resulting from eccentric traffic. The deck girder and pylons are often monolithically connected. This way, the short pylon can be slender and stabilized against buckling more economically than through cables. For the version of the torsionally not rigid bridge deck, it is necessary to ensure stability using two planes of cables. The monolithic connection between the pylon and the deck girder further improves robustness and durability, but a bridge bearing is also used. Some extradosed bridges are fully integral, that is, the deck girder and piers are also monolithically connected.

Neglecting the costs of the bridge pylons, deck girders of extradosed bridge are often cheaper than the deck girders of a girder bridge. This is due to the concrete being the principal ingredient in the superstructure cost, so that extradosed bridges become more efficient with increasing span. While the presence of pylons and stay cables of extradosed bridges poses additional costs compared to post-tensioned cantilever bridges, shorter height of the pylons and adoption of saddles instead of anchorages increase their economy over those used for traditional cable-stayed bridges.

Indeed, there is a design freedom into varying the relative stiffness of the deck, cables, and pylons to optimize the behaviour of the bridge. This results in a range of structural characteristics in between an internally post-tensioned balanced cantilever bridge and a cable-stayed bridge, with ample room for innovation and reducing cost for different boundary conditions and design restriction. As noted above, unlike cable-stayed bridges, extradosed bridges do not require back stays to limit the horizontal movement at the top of the pylon caused by uneven live loads, when the short pylon is monolithically fixed to the deck because the live loads are primarily carried in bending by the deck girder. Thus, extradosed bridges are inherently well suited to multi-span structures [1].

2.1. Pylons

The pylon's height measured above the bridge deck level is between $0.07L$ and $0.13L$, where L denotes the lenght of the main span. This is considerably shorter than in the classic cable-stayed bridges, where the pylon has a height between $0.2L$ and $0.25L$, which explains why the pylons are easier to build for extradosed bridges. Having this geometrical arrangement, extradosed bridge stays are slightly inclined with respect to the roadway and, therefore, provide

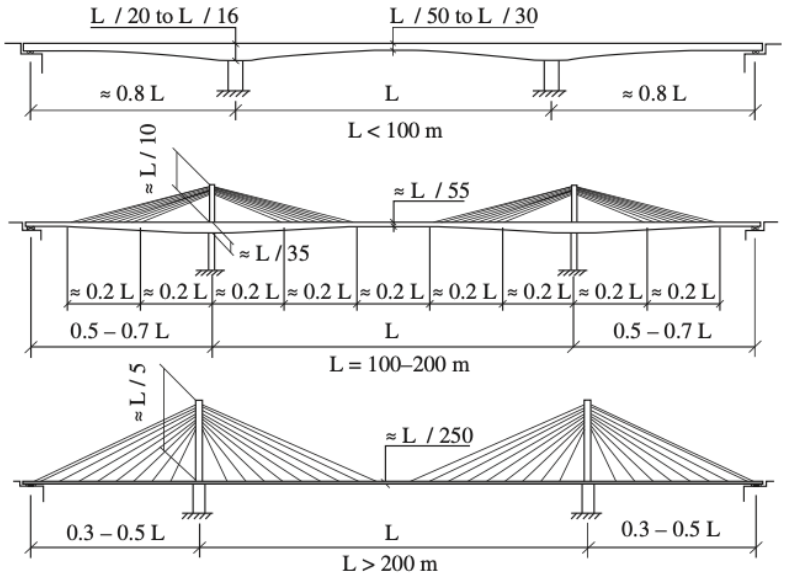

FIGURE 1. Comparison of three bridges with different dimensions [1].

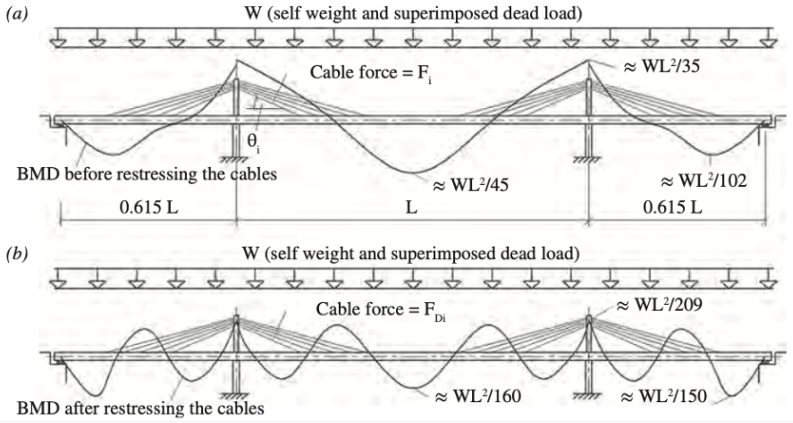

FIGURE 2. BMD (Bending Moment Deformation) before and after the restressing of cables under dead load [1].

smaller vertical stiffness to the deck when compared to cable-stayed bridge. The stays are often anchored and closely spaced in groups that subdivide the main span length L into portions of $0.2L$ [1].

2.2. DECK

Most extradosed bridges that have been built so far have stiffer and stronger girders in bending compared to cable-stayed bridges. Desks generally carry live loads primarily in bending. For girders of constant thicknesses, typical are among $L/40$ to $L/45$. The elegant Sunniberg Bridge by Christian Menn in Switzerland, with its slender concrete slab deck, is certainly an exception that sets the current trend and serves as the inspiration for this work. The ratio of the thickness of the deck to the main length of the field for the Sunniberg bridge is up to $L/250$, which cannot be applied in all cases, but it is a challenge for saving material [1, 2].

2.3. CABLES

Thanks to reduced fatigue due to the lower stress range in the stay cables, they can be subjected to higher stress, allowing for the use of simpler and more economical anchorages. For the same reason anchorages of extradosed bridges are typically subject to fatigue test requirements, which are less demanding than those for cable-stayed bridges [1, 3].

All these properties that are disadvantageous to cable-stayed bridges result in live loads that are carried by the deck and, therefore, result in small stress changes in the cables. The cables of extradosed bridges are mainly present to carry permanent loads, reducing so the bending moments in the deck (Figure 2). The small stress changes in the cables due to live loads reduce the risk of fatigue failure and, therefore, the utilization of the cables can be higher than 45 % of the Guaranteed Ultimate Tensile Strength (GUTS) which is usually applied for cable- stayed bridges. This represents a better use of the cable capacity in service compared with cable-stayed bridges (Figure 3). How-

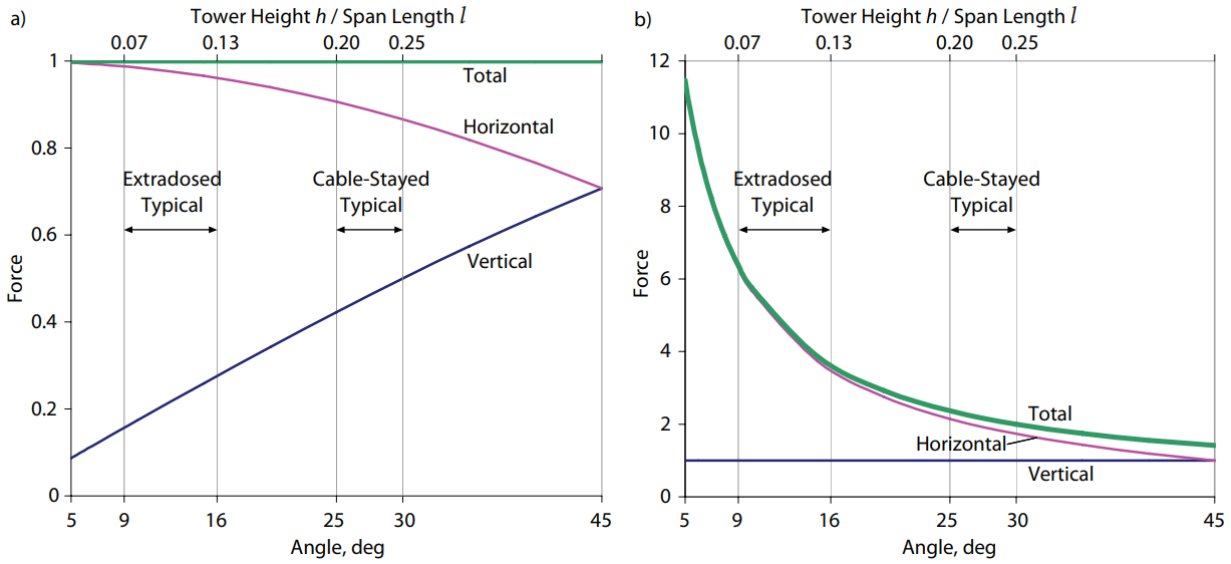

Figure 3. Effect of cable inclination on the force components in a cable for a) a constant total force and b) a constant vertical force [4].

ever, rather than simply raising the allowable stress to 60 % of GUTS, for example, it is desirable to provide structural rationale. A thorough investigation of many existing bridges confirms that there is no clear boundary between extradosed and cable-stayed bridges and shows that the maximum allowable stresses in service should be based on the level of stress changes due to live loads [1]].

2.4. Non-linear cable analysis

In the case of rope elements, their stiffness is reduced due to their sag. Thus, the replacement modulus of elasticity is reduced. The introduced normal force is partly exhausted by changing the geometry of the element until the moment when the rope is diminished. Since then, it can be assumed that the element behaves linearly and the full stiffness of the rope acts. This behavior is generally referred to as tension stiffening (Figure 4) [5]. Stress stiffening, also known as geometric stiffening, incremental stiffening, initial stress stiffening, or differential stiffening according to various authors, refers to the increase (or decrease) in the stiffness of a structure due to its stress condition. This phenomenon is particularly relevant in thin structures where bending stiffness is significantly smaller compared to axial stiffness, such as cables, thin beams, and shells, and it couples the in-plane and transverse displacements. Additionally, stress stiffening complements the conventional nonlinear stiffness matrix resulting from large-strain or large-deflection effects. To account for stress stiffening, an extra stiffness matrix, referred to as the geometric stiffness matrix K_g is computed and incorporated into the overall stiffness matrix [6].

Where l is the horizontal length of the rope anchorage, h is the vertical height of the rope anchorage, s is the rope length, α is the angle of inclination, H are the

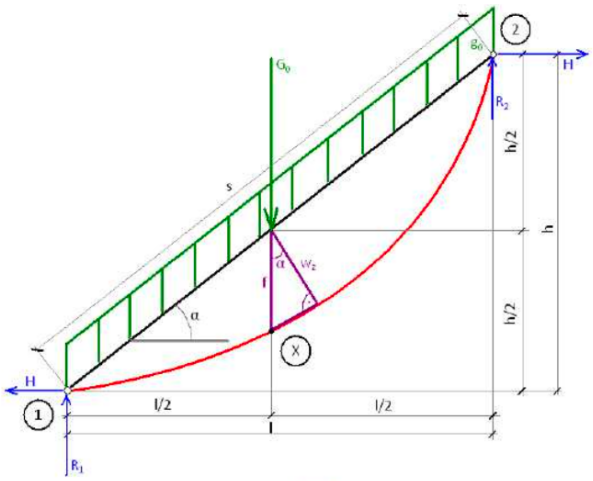

Figure 4. Non-linear behaviour analysis of the bridge cable [5].

horizontal reaction forces, R_1 and R_2 the vertical reaction forces, g_0 is the dead load of the rope, G_0 is the resultant force, f is the vertical sag of the rope, and w_z is the perpendicular sag, which is approximately.

$$w_z \approx f \cos \alpha. \tag{1}$$

The deformable conditions of this calculation are the initial length of the rope $L_0 = s$ and the length of the parabola, which is length of the sagged rope. Assuming a simplification, the sag of the rope will not have the catenary shape, but will have a parabolic course. The length of the parabola is then calculated as

$$L_p \doteq s \left(1 + \frac{8 w_z^2}{s^2}\right). \tag{2}$$

The rotational equilibrium condition in point 1 is

$$R_2 l - \frac{G_0 l}{2} - Hl = 0. \tag{3}$$

Equilibrium condition of all vertical forces:

$$R_1 + R_2 - G_0 = 0. \tag{4}$$

The rotational equilibrium condition in point X

$$\frac{R_1 l}{2} + H\left(\frac{h}{2} - f\right) - \frac{g_0 s}{2} \cdot \frac{l}{4} = 0. \tag{5}$$

From the system of equations, we obtain the value of the horizontal reaction H at the anchorages, in which f figures as unknown variable

$$H = \frac{G_0 l}{8f}. \tag{6}$$

Variance of geometric extension caused from self weight is calculated as

$$\Delta L_s = L_p - L_0, \tag{7}$$

$$\Delta L_s = s\frac{8f^2}{3\theta^4 l^2}, \tag{8}$$

where these geometric constants figure

$$\theta = \frac{1}{\cos\alpha}. \tag{9}$$

Change of extension by the force in the rope from the attachment calculated as

$$\Delta L_N = \frac{N}{E_p A_p} s, \tag{10}$$

where N is the force in the rope, E_p is the Young's modulus of the material and A_p is the cross-sectional area of the rope. Relationship between the force N and horizontal reaction H is

$$N = \frac{H}{\cos\alpha}. \tag{11}$$

The total extension outgoing from geometric and force in the rope must be the equal. By substituting Eqs. (8), (11) and (12) into the equation

$$\Delta L_N = \Delta L_s. \tag{12}$$

We get

$$\frac{sH}{E_p A_p \cos\alpha} = s\frac{8f^2}{3\theta^4 l^2}. \tag{13}$$

Further, substituting Eq. (6) into Eq. (14)

$$\frac{G_0 l}{8f E_p A_p \cos\alpha} = \frac{8f^2}{3\theta^4 l^2}. \tag{14}$$

After modifying the equation, we get an expression for the rope sag without pretension

$$f = \sqrt[3]{\frac{G_0 l^3 \theta^4}{E_p A_p} \cdot \frac{3}{64}}. \tag{15}$$

The change in extansion from a prestressing force N_p is

$$\begin{aligned} \Delta L_N &= s\left(\frac{N}{E_p A_p} - \frac{N_p}{E_p A_p}\right) \\ &= s\left(\frac{G_0 l}{8f E_p A_p \cos\alpha} - \frac{N_p}{E_p A_p}\right). \end{aligned} \tag{16}$$

By substituting Eqs. (8) and (11) back into Eq. (13) we get a cubic equation for calculating rope sag f depending on the prestressing force N_p

$$f^3\left(\frac{8}{3\theta^4 l^2}\right) + f\left(\frac{N_p}{E_p A_p}\right) - \frac{G_0 l}{8E_p A_p \cos\alpha} = 0. \tag{17}$$

By calculating the sag f, all forces related to the rope can be count backwards. In the end the parameter used further in the matrix of stiffness of the cable elements representing the non-linear behaviour of the cable is the reduced effective Young's modulus E_{eff} [7].

$$E_{\text{eff}} = \frac{E_P}{1 + \frac{\gamma^2 l_c^2 E_P}{12\sigma^3}} \tag{18}$$

Where σ is the tensile stress in the cable, γ is the volumetric weight of the cable, l_c is the horizontal projection of the length of the cable. All the variables for calculating the length of the rope in Eq. (2) are solved. This calculation in combination with Eq. (19) are the essentials parameteres for correct usage of non-linerar behaviour in the coputional analysis of the bridge cables [5].

3. FEM model

Based on the large amount of bridge data and case studies from 2019 provided by IABSE [1], approximately 59 % of extradosed bridges have two pylons in longitudinal direction, i.e. three spans, 19 % have one pylon and two spans, and the remaining 22 % have three or more pylons. The research deals only with the most widespread variant, so the option of a 3 fields bridge with 2 pylons is modeled here.

3.1. Description of the model

The description of the model is simplified by using three basic component types: deck, pylon and cable [8]. The predescribed size of spans and pylons is divided into nodes according to the required density. Due to the fact that the segments are usually 5 m, the nodes are in the same grid. Generated nodes and finite elements are described in the planar coordinate system. The elements modeling the cables that connect the pylon and bridge deck are made up of one piece element [7]. The geometric nonlinearity of the cables is captured using the effective Young's modulus (19) [8]. For each finite element, a local stiffness is built based on the nodal coordinates utilizing the

relevant geometric and material characteristics. The local matrices are then transformed into the global coordinate system using a transformation matrix. The localization of the matrices into the global matrix takes place using code numbers [9, 10]. The numerical model employs Euler-Bernoulli frame elements with three degrees of freedom at each node, resulting in a stiffness matrix represented as a 6×6 matrix for each element.

$$K_e = \frac{E}{L} \begin{pmatrix} A & 0 & 0 & -A & 0 & 0 \\ 0 & \frac{12I}{L^2} & -\frac{6I}{L} & 0 & -\frac{12I}{L^2} & -\frac{6I}{L} \\ 0 & -\frac{6I}{L} & 4I & 0 & \frac{6I}{L} & 2I \\ -A & 0 & 0 & A & 0 & 0 \\ 0 & -\frac{12I}{L^2} & \frac{6I}{L} & 0 & \frac{12I}{L^2} & \frac{6I}{L} \\ 0 & -\frac{6I}{L} & 2I & 0 & \frac{6I}{L} & 4I \end{pmatrix}, \quad (19)$$

where

E is Young's modulus of the material [kPa],

I is the moment of inertia for the Y-axis in base of the cross-section [m^4],

A is the element area [m^2],

L is the lenght of the element [m].

Further, the geometric stiffness reads as

$$K_g = \frac{P}{30L} \begin{pmatrix} 0 & 0 & 0 & 0 & 0 & 0 \\ 0 & 36 & 3L & 0 & -36 & 3L \\ 0 & 3L & 4L^2 & 0 & -3L & -L^2 \\ 0 & 0 & 0 & 0 & 0 & 0 \\ 0 & -36 & -3L & 0 & 36 & -3L \\ 0 & 3L & -L^2 & 0 & -3L & 4L^2 \end{pmatrix}, \quad (20)$$

P is the stressing/tension force in the element [kN].

Prestressing forces in the cables are defined as vector of variables

$$P = (P_1, P_2, P_3, \ldots, P_n), \quad (21)$$

where n is the number of cables. Each cable is digitized using also a vector

$$C = (C_1, C_2, C_3, \ldots, C_n). \quad (22)$$

Forces are assigned to cables with the same index.

The local stiffness matrix further consists of

$$K_L = K_e + K_g. \quad (23)$$

Finally the element matrixes are transformed into the global coordinate system using the transformation matrix

$$T = \begin{pmatrix} \cos\alpha & \sin\alpha & 0 & 0 & 0 & 0 \\ -\sin\alpha & \cos\alpha & 0 & 0 & 0 & 0 \\ 0 & 0 & 1 & 0 & 0 & 0 \\ 0 & 0 & 0 & \cos\alpha & \sin\alpha & 0 \\ 0 & 0 & 0 & -\sin\alpha & \cos\alpha & 0 \\ 0 & 0 & 0 & 0 & 0 & 1 \end{pmatrix} \quad (24)$$

$$K_G = T' K_L T, \quad (25)$$

K_G is the global stiffness matrix.

3.2. Kinematic boundary conditions of nodes

At each end of the deck, there are free rotation and horizontal displacements that represent the movement of the expansion joints and bearings. The element intersection of the pylon and the deck is fundamental for the overall behaviour of the bridge. Further, there are two variants: one maintains a rigid (monolitic) connection, while the other support one is supported by bearings. The anchoring places of the cables are also different. They can be expected to rotate around a joint, or the place is fixed in such a way that rotation is prevented. In this case the entire structure is supported on bearings and the cables are on pivots allowing rotation.

3.3. Load/force vector

The cables are typically designed to carry 60–80 % of the dead loads, which represent the dominant part of loading. The rest of the dead load, with the increment from the moving load from vehicles or trains, is carried by the deck. The deck weight is generated in the nodes as a load calculated according to the geometry and density of the material. For the purposes of this work, the dead load is the only load case.

3.4. Limiting conditions and objectives

The condition for Serviceability Limit State (SLS) is the limitation of this task. The maximum deck deformation is limited to $L/600$ for prestressed bridges. Cable-stayed bridges are prestressed usually at 45 % of their characteristic strengths due to major live load stress change. In girder, this limit is extended to 60 %. Extradosed bridges are somewhere in between. Therefore the cable prestress range is usually between 45 % and 60 % of the characteristic strength [1].

3.5. Model simplification

Mathematical and material models try to describe reality as accurately as possible, yet sometimes achieving a small accuracy requires a large effort that is not conventional.

3.5.1. Cable anchorage-change in sag, strength and modulus of elasticity

From a construction point of view, it is very difficult and sometimes even impossible to have the pylon anchorages close to each other. Anchoring is usually approximately 1–5 m apart, according to the technical requirements for anchoring. The purpose of this optimization program is to generate a number of cables from the top of the pylon for the desired results. The problem requires define the next cables are located far enough from each other, because this creates a lot

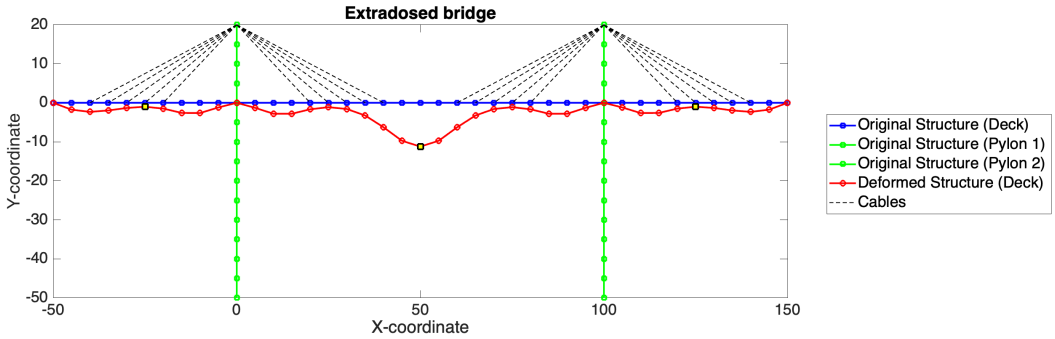

FIGURE 5. Deflection of the extradosed bridge with the span of the main bridge $L = 100\,\text{m}$. Scale factor $\times 100$.

of extra nodes that must be defined correctly. An effective and advantageous solution can be that all the cables are connected to the pylon at one point (we can call it the saddle of the pylon) and thus create a fan. From a construction point of view, this solution is impractical, but from a numerical analysis point of view, it is ideal for describing cables. In principle, it is a change in the hinge angle. However for a 100–250 m field, the difference is about 1–5 m in the vertical direction, so it has a little effect on the redistribution of the prestressing force in the horizontal and vertical directions.

3.5.2. Cross-section variability

The variability of the cross-section is typical for these types of construction. The pylon usually has a larger cross-section (the so-called pierhead) for better load-bearing capacity and rigidity, while the cross-section in the field is thinner to reduce the self-weight load. The finite elements are generated along the length of the bridge deck with a constant cross-section. An average ideal cross-section is assumed. This simplification is not expected to have a major impact on the results.

3.5.3. Level of the bridge

The level of the bridge deck will be considered zero, with no longitudinal slope. This will have a negligible effect on the calculation.

3.6. Static analysis

Geometric and material characteristics similar to those of the Sunniberg bridge were used as a model example: rectangular slab bridge with dimensions of $8 \times 0.5\,\text{m}$, concrete type C40/50 and 2 rows of cables with a diameter of 0.2 m [2]. The static response depends on the structure's stiffness and the load's size. This is expressed using the equilibrium equation

$$Ku = f, \tag{26}$$

in which K is the global stiffness matrix, u is the displacement vector and f is the force vector. Deflection u of the deck is calculated and depicted is comparison to the original not deformed structure (Figure 5).

The maximal deflection without prestressing forces in the cables $u_{0,100}$ appear to be in the middle of the span $u_{0,100} = 0,112\,\text{m}$.

The deformation of the deck is limited by $u_{\max}$ for prestressed concrete structures [11], where the limiting value is set as

$$u_{\max} = \frac{L}{600} \tag{27}$$

with L denoting the lenght of the span in meters. For the the main span $L = 100\,\text{m}$ is the the maximal deflection $u_{\max,100} = 0.166\,\text{m}$.

The deflection is clearly under the deflection limit. Even so, taking into account the live load or with a larger field span, the prestressing forces in the cables must be set.

4. Optimalization function

Function *fmincon* is a Matlab inbuilt nonlinear programming optimizer that finds a minimum of constrained nonlinear multi-variable function [12]. Described as finding the minimum of a problem specified by:

$$\begin{aligned} \text{minimize} \quad & f(x) \\ & c(x) \le 0 \\ & ceq(x) = 0 \\ \text{subject to} \quad & A \cdot x \le b \\ & A_{eq} \cdot x \le b_{eq} \\ & lb \le x \le ub. \end{aligned} \tag{28}$$

The function $f(x)$ is the deck deflection u in this case. Deflection is monitored at 3 control points, namely the nodes in the middle of each field. The lower bound l_b is a vector of zeroes, this represents the possibility of no force in the cables. The upper bound u_b is the vector of maximum forces $F_{\max}$, which is the maximum allowable force deriving the maximum allowable tension in the cable. The result of the optimization is the force vector for the cables, which derives the minimum function $f(x)$, i.e. the smallest deflection in the 3 monitored points.

5. Results

The force vector obtained from the optimization was inserted into the structure calculation and the deflection in the middle was reduced after prestressing to $u_{F,100} = 0.048\,\text{m}$ (Figure 6).

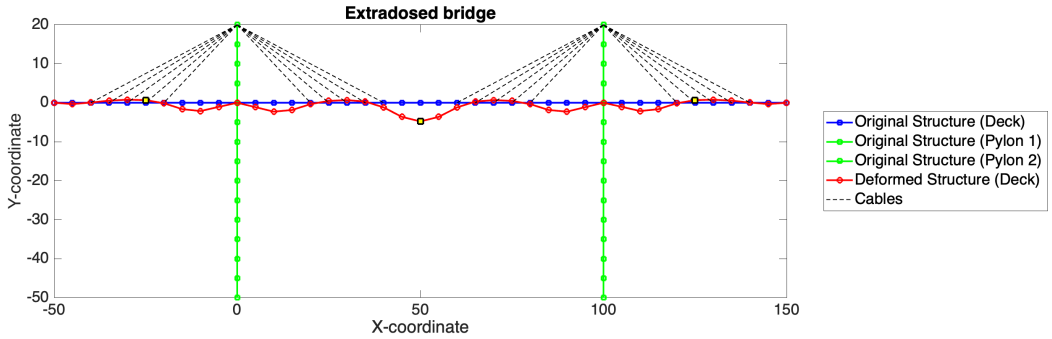

Figure 6. Deflection of the extradosed bridge with the span of the main bridge $L = 100\,\text{m}$ after prestressing. Scale factor $\times 100$.

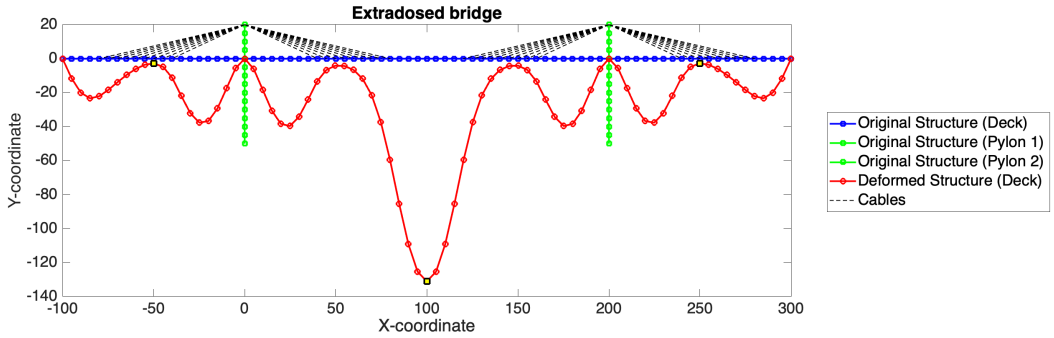

Figure 7. Deflection of the extradosed bridge with the span of the main bridge $L = 200\,\text{m}$. Scale factor $\times 100$.

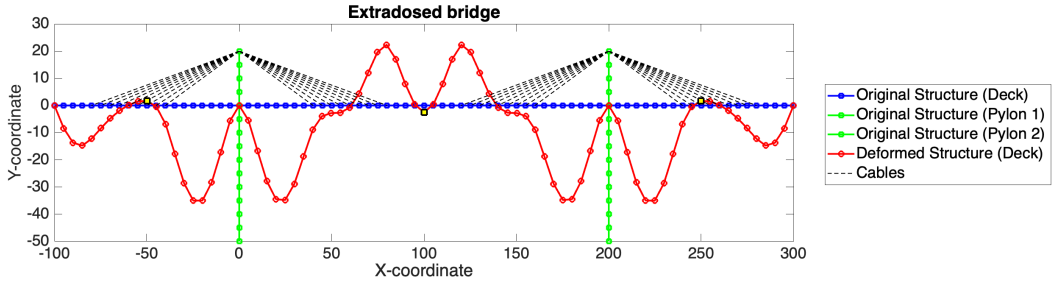

Figure 8. Deflection of the extradosed bridge with the span of the main bridge $L = 200\,\text{m}$ after prestressing. Scale factor $\times 100$.

Variants of the extradosed bridge with main spans of 120 m, 140 m, 160 m, 180 m and 200 m were also tested for research purposes, each of them having a adequate number of cables (200 m variant has a set of 36 pairs of cables due to its dimensions). For example, the deflection of the 200 m long main span of the bridge is without prestressing $u_{0,200} = 1.311\,\text{m}$ (Figure 7). For the the main span $L = 200\,\text{m}$ is the the maximal deflection $u_{\max,200} = 0.333\,\text{m}$.

The deflection is clearly upper the deflection limit, the prestressing forces in the cables must be set to achieve the deflection limit. After optimizing the forces in the cables, the deflection in the middle of the deck is reduced to $u_{F,200} = 0.025\,\text{m}$ (Figure 8).

The results in terms of magnitude of forces derived from the optimization for different sizes and numbers of cables are shown in the graph (Figure 9).

6. Conclusions

The research shows that as the length of the main span increases, significantly greater force is required to lift the cables closer to the center of the main span, in order to reach the maximum vertical deflection limit. This indicates that not all cables are fully utilized in the current arrangement, and as the length of the main span increases, a different cable distribution may be required (see Figure 10).

For larger spans, a more uniform distribution of cables along the bridge deck is preferable, which may also require an increased number of cables. This, in turn, necessitates additional space for anchoring the cables to a taller pylon, making the structure more similar to a cable-stayed bridge.

Such a design calls for a more detailed analysis considering variable live loads [13], further evaluation in terms of limit states, local analyses at several points along the bridge deck, and optimization of the pylon

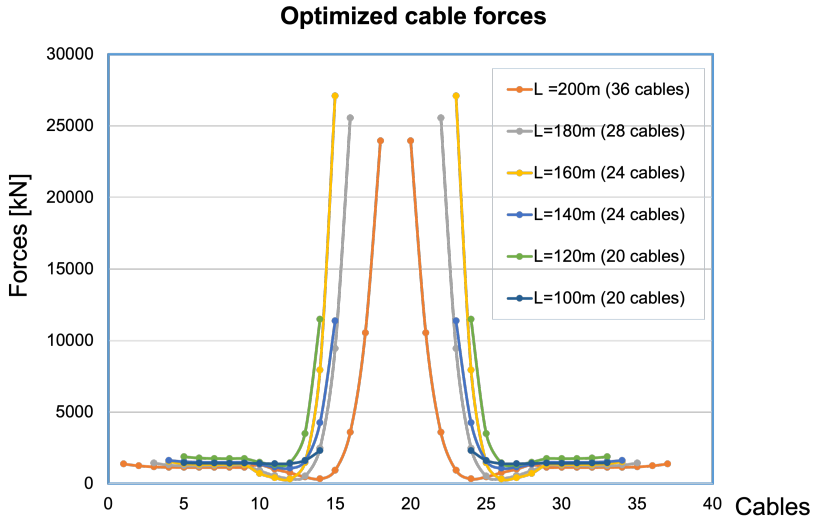

FIGURE 9. Optimized cable forces – 2D graph.

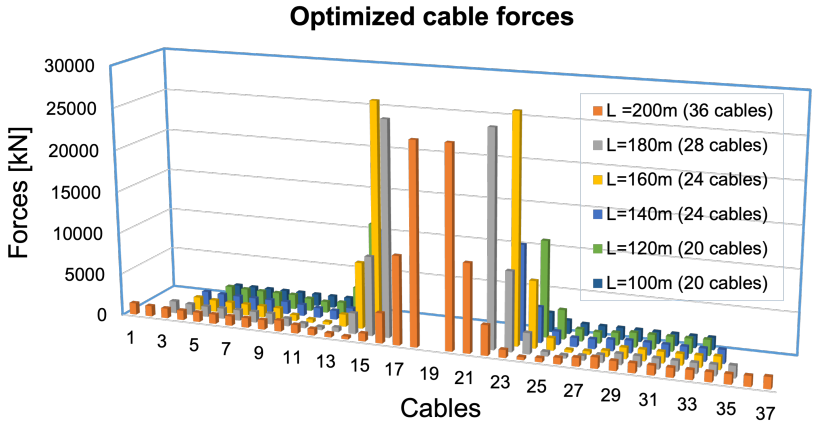

FIGURE 10. Optimized cable forces – 3D graph.

height. The height of the pylon is a critical factor not only for determining the type of bridge but also for its economic feasibility.

ACKNOWLEDGEMENTS

The authors gratefully acknowledge support from the Czech Technical University in Prague, project SGS23/032/OHK1/1T/11 Development and application of numerical algorithms for analysis and modelling in mechanics of structures and materials.

REFERENCES

[1] Structural Engineering Documents (SED) 17. *Extradosed Bridges*. IABSE Bulletins, 2019. ISBN 978-3-85748-168-0, [2024-02-01]. `https://concrete.ethz.ch/assets/sed17.pdf`

[2] C. Menn. Sunniberg Bridge, 2024. [2024-02-01]. `https://www.bridgeinfo.net/bridge/index.php?ID=241`

[3] F. Faltus. *Ocelové mosty příhradové, obloukové a visuté [In Czech; Steel Bridges – Truss, Arch and Suspension Structures]*. Praha: Academia, 1971.

[4] K. K. Mermigas. *Behaviour and Design of Extradosed Bridges*. Master's thesis, University of Toronto, 2008.

[5] L. Vráblík. Computational analysis of a cable stayed bridge structure, 2021. Lecture.

[6] Z. Bittnar, J. Šejnoha. *Numerické metody mechaniky I [In Czech; Numerical Methods in Mechanics I]*. Czech Technical University in Prague, 1992. xxi+634 p. ISBN 80-01-00855-X.

[7] J. Yi. Modeling and analysis of cable vibrations in cable-stayed bridges under near-fault ground motions. *Engineering Structures* **277**:115443, 2023. `https://doi.org/10.1016/j.engstruct.2022.115443`

[8] R. Šafář. *Betonové mosty 2.: Přednášky [In Czech; Concrete Bridges 2: Lectures]*. Czech Technical University in Prague, 2017. ISBN 978-80-01-05543-4.

[9] K. D'Amico. Dynamic behavior of cable-stayed footbridge depending on the calculation accuracy. In *Conference Nano and Macro Mechanics (NMM2023)*. Czech Technical University in Prague, 2023. [2024-02-01]. https://mech.fsv.cvut.cz/nmm2023/en/

[10] Z. Bittnar, P. Řeřicha. *Metoda konečných prvků v dynamice konstrukcí [In Czech; Finite Element Method in Structural Dynamics]*. SNTL Praha, 1981.

[11] Czech Office for Standards, Metrology and Testing. *Navrhování betonových mostních konstrukcí [In Czech; Design of Concrete Bridge Structures]*, 2014. ČSN 73 6214.

[12] M. Tyburec. *Modular-topology optimization of structures and mechanisms*. Ph.D. thesis, Czech Technical University in Prague, 2021. [2024-02-01]. https://dspace.cvut.cz/handle/10467/98774

[13] Czech Office for Standards, Metrology and Testing. *Eurocode 1: Actions on Structures – Part 2: Traffic Loads on Bridges*, 2018. ČSN EN 1991-2 ed. 2 (73 6203).